Catal Lett (2009) 130:1–8
DOI 10.1007/s10562-009-9894-1

Fe-BEA Zeolite Catalysts for NH_3-SCR of NO_x

Anne Mette Frey · Selcuk Mert · Johannes Due-Hansen · Rasmus Fehrmann · Claus Hviid Christensen

Received: 11 November 2008 / Accepted: 4 February 2009 / Published online: 24 February 2009

Abstract Iron-containing zeolites are known to be promising catalysts for the NH_3-SCR reaction. Here, we will investigate the catalytic activity of iron-based BEA catalysts, which was found to exhibit improved activities compared to previously described iron-containing zeolite catalysts, such as ZSM-5 and ZSM-12. Series of Fe-BEA zeolite catalysts were prepared using a range of different preparation methods. Furthermore, we found that an iron concentration around 3 wt% on BEA showed a small optimum in SCR activity compared to the other iron loadings studied.

Keywords NH_3-SCR · NO_x · Fe-BEA · Zeolite catalysts

1 Introduction

Nitrogen oxides, NO_x, are formed during combustion of nitrogen-containing fuels in stationary as well as automotive applications. The transportation sector is one of the major source of NO_x formation and it contributes to 20% of the total global emission of NO_x [1, 2]. Legislation is steadily leading to lowering of the acceptable NO_x concentrations in the exhaust of vehicles in EU-countries, US, and Japan. This makes it necessary to improve and develop methods to remove NO_x efficiently from the exhaust gases in automotives. The most efficient way to remove NO_x is by the selective catalytic reduction process using ammonia as the reductant and it seems to be the most efficient technique to meet future NO_x emission standards for mobile applications. The method has already been used extensively in stationary applications since the 1970s. Accordingly, the reaction will be considered in more detail here. In the NH_3-SCR process, ammonia or urea is injected into the exhaust gas prior to the catalyst [3]. The over-all catalytic reaction, which takes place is [5]:

$$4NO + 4NH_3 + O_2 \rightarrow 4N_2 + 6H_2O. \quad (1)$$

However, if equimolar amounts of NO and NO_2 are present in the exhaust gas, the process can be accelerated in a reaction known as fast SCR [4],

$$2NO + 2NO_2 + 4NH_3 \rightarrow 4N_2 + 6H_2O. \quad (2)$$

In automotive applications, vanadium-based catalysts are often used as catalysts for the NH_3-SCR reaction [5, 6]. However, catalysts containing vanadium have several drawbacks when used for this application. Poisonous vanadium can be lost during the process and released into the environment, the catalyst exhibits low activity at low temperatures, and a low selectivity is observed at high temperatures due to competitive ammonia oxidation. Furthermore, the vanadium catalysts are active in the oxidation of SO_2 to SO_3. Due to these problems, it is desirable to develop other types of NH_3-SCR catalysts.

During the last 20 years, much research has been carried out concerning zeolite catalysts for the NH_3-SCR reaction. Different zeolite materials, such as MOR, MFI, Y, BEA, FER loaded with various metals, i.e. Cu, Co, Fe and Pt, have been investigated [7–10].

Electronic supplementary material The online version of this article (doi:10.1007/s10562-009-9894-1) contains supplementary material, which is available to authorized users.

A. M. Frey · S. Mert · J. Due-Hansen · R. Fehrmann (✉)
Department of Chemistry, Center for Sustainable and Green Chemistry, Technical University of Denmark, 2800 Lyngby, Denmark
e-mail: rf@kemi.dtu.dk

C. H. Christensen
Haldor Topsøe A/S, Nymøllevej 55, 2800 Lyngby, Denmark

Especially, copper-based zeolites have been examined thoroughly because these materials were the first metal zeolites found to be active in SCR. Cu-zeolites are found to be active both when using HC and NH_3 as reducing agents [4, 11]. As an example, it can be mentioned that a 2.4 wt% Cu-ZSM-5 was claimed to be more active than a conventionally prepared V_2O_5/TiO_2 catalyst in the SCR of NO_x with NH_3 [12]. Though these catalysts originally seemed promising, Cu-based catalysts are not very attractive for automotive applications due to their limited hydrothermal stability—the presence of water in the exit gas can quickly poison the catalyst severely [13]. This means that other possibilities must be considered and among all the metal-zeolite catalyst systems tested to this point iron catalysts seem to be the most promising. So far, it is Fe-ZSM-5 catalysts that have been the most studied SCR catalyst in terms of preparation, characterization and catalytic performance among the Fe-zeolite systems [14–16].

An interesting and promising system is the Fe-BEA catalyst system. Early SCR studies of the zeolite beta system have been performed by Delahay et al., especially on the reduction of N_2O by NH_3-SCR [7], but the authors have not investigated the performance of Fe-BEA in the SCR of NO.

In this work, we have compared Fe-BEA to Fe-ZSM-5 and Fe-ZSM-12. We found, that Fe-BEA indeed was superior in NO reduction to the other zeolite catalysts in a very broad temperature interval. The Fe-BEA catalysts exhibit even higher activity than a typical vanadium anatase catalyst. Based on these results we have prepared iron-containing BEA zeolites in different ways, and thereby studied the influence of the preparation method on the NO reduction in the NH_3-SCR reaction. Furthermore, we have determined the optimal iron content in these samples.

2 Experimental Section

2.1 Catalysts Preparation

Several series of iron containing catalysts using different zeolite materials were prepared. Here, we will focus on the preparation of the Fe-BEA catalysts. Information regarding preparation of iron-containing ZSM-5 and ZSM-12 zeolites is described elsewhere [17].

Two series of catalysts were prepared first by synthesizing the H-BEA zeolite followed by a second step in which the introduction of the iron took place by either incipient wetness impregnation (IWI) or by ion exchange (IE) techniques. Another series of catalysts were prepared by isomorphous substitution (IS) of iron into the zeolite framework during the zeolite synthesis.

2.1.1 Zeolite Preparation

2.1.1.1 Na-BEA To produce approximately 10 g of a conventional Na-BEA zeolite, the following recipe was applied:

About 3.5 g of $NaAlO_2$ was dissolved in 25 mL of water and added dropwise to 1.5 g of NaOH dissolved in 10 mL of water while stirring. The stirring was continued for 10 min. About 30 g of SiO_2 (Sigma-Aldrich Silica Gel, grade 62, 60–200 mesh, 150 Å) was then added slowly under stirring followed by addition of 92 g of a 40 wt% tetraethylammonium hydroxide (TEAOH) solution, and the suspension was stirred for additional 2 h. The resulting gel was transferred to an autoclave, sealed and heated to 140 °C for 120 h. After the crystallization period the autoclave was quenched in cold water. The product was filtered and washed thoroughly with water until pH = 8 were reached in the filtrate (approximately 2 L of water). The sample was dried at room temperature overnight, followed by 30 min of drying at 110 °C. In order to remove the template, the sample was calcined at 550 °C (~2 °C/min) for 18 h in air, resulting in a white powder.

2.1.1.2 NH_4-BEA To obtain the corresponding NH_4-BEA zeolite, the Na-BEA zeolite was treated with 1 M NH_4NO_3 (1:30 g/g) for 4 h at 80 °C during stirring. The zeolite was filtered and washed with 2 L water and dried. The following day the ammonium nitrate treatment, filtration, washing and drying steps were repeated.

2.1.1.3 H-BEA The H-BEA zeolite was obtained by heating the NH_4-BEA to 450 °C (3.5 °C/min) for 4 h. All samples were pressed into tablets under a pressure of 5 tons (Ø = 13 mm), crushed and sieved to obtain a particle size of 180–355 μm. After that, the zeolite fraction was ready for the introduction of iron.

2.1.2 Introducing Iron to the Samples

2.1.2.1 Incipient Wetness Impregnation (IWI) The zeolite was impregnated with a solution of $Fe(NO_3)_3 \cdot 9H_2O$ in water, containing the amount of iron needed to obtain the desired iron content in the samples. Samples containing 1.0, 2.0, 2.7, 3.0, 3.5, and 5.0 wt% iron were prepared. After impregnation, the samples were left for 1 h in a closed container in order to get the metal ions evenly distributed in the zeolite. Then, the samples were dried overnight at room temperature. The drying procedure was followed by a calcination step, in which the samples were heated in air from room temperature to 450 °C (3.5 °C/min) for 4 h.

2.1.2.2 Conventional Ion Exchange (IE) About 1.25 g of H-BEA was added to 0.5 L of a 2 mM iron (III) nitrate

solution and stirred for 48 h. The suspension was filtered and the product was washed three times with 0.5 L of water followed by drying at 80 °C for 2 h. The samples were then calcined at 450 °C (5 °C/min) for 4 h.

2.1.2.3 Isomorphous Substitution (IS) The main difference from this synthesis and the zeolite synthesis described above is that the iron is introduced directly into the gel during the synthesis of the IS sample. This was done by substituting aluminium partly or fully by iron in the recipe. Samples with two different iron contents were prepared. One where 50% of the aluminium was substituted by iron (described below) and one where all aluminium was substituted by iron (prepared analogously but with twice as much iron added and without aluminium).

Two solutions were prepared to synthesize a sample where 50% of aluminium was substituted by iron.

A: 0.28 g of NaOH was dissolved in 3.5 mL of water and mixed with a solution containing 0.79 g of $NaAlO_2$ in 5 mL of water. Finally 11.90 g of a 40 wt% TEAOH solution was added.

B: A solution of 0.45 g $Fe(NO_3)_3 \cdot 9H_2O$ in 5 mL water was poured into 11.90 g of a TEAOH solution.

Solutions A and B were then simultaneously poured onto 7.5 g of SiO_2 during vigorous stirring and the stirring was continued until a red homogenous gel was obtained.

The gel was transferred to a stainless steel autoclave, sealed and heated to 120 °C, and left there for 140 h. The autoclave was then cooled to room temperature, opened, filtered and the product was washed three times with water until the washing water was neutral, followed by drying for 1 h at 120 °C. After the drying procedure the sample was calcined in air at 550 °C (~2 °C/min) for 18 h. The resulting zeolite was converted to the NH_4-form by mixing the sample with 1 M NH_4NO_3 (1:30 g/g) and stirring for 3 h at 80 °C. Thus, the sample was thoroughly washed with water and dried over night at room temperature. The ion-exchange and washing steps were repeated the following day and the sample was calcined at 450 °C (5 °C/min) for 4 h to obtain the zeolite in the H-form.

2.2 Catalytic Activity Tests

The activity tests were in all cases performed with 50 mg catalyst, fractionated to 180–355 μm, in an isothermal fixed bed quartz reactor, with a diameter of 3.8 mm, operated under plug-flow conditions. The catalyst was pretreated at 200 °C for 15 h followed by 2 h of activation in the reactant gas consisting of 1000 ppm NO, 1100 ppm NH_3, 2.3% H_2O and 3.5% O_2 balanced with N_2 to a total flow of 300 mL/min (ambient conditions). After pretreatment, the reactor was cooled to room temperature. The activity was then measured multiple times at selected temperatures from 200 to 550 °C using a Thermo Electron's Model 10A chemiluminiscent NO-NO_x Gas Analyzer to measure exit gas compositions.

2.3 Characterization Techniques

XRD patterns of all samples were recorded using a Bruker powder diffractometer with Cu-$K_{\alpha 1}$ radiation (λ = 1.54051 Å) in the 2θ interval of 1–60° in steps of 0.02°.

ICP-MS in SemiQuant Mode was used to determine the iron content in the samples. A calibration curve was obtained from a Merck ICP multi element standard solution.

N_2 adsorption measurements were performed at liquid nitrogen temperature on a Micromeritics ASAP2020 analyzer. In all cases, the samples were evacuated at 200 °C for 1 h prior to the measurement. Based on these measurements, the micropore volume and the surface areas were determined by the t-plot method [18] and the BET methods [19], respectively.

Temperature programmed desorption (TPD) of ammonia were performed in the following way: 100 mg of catalyst sample was loaded into a quartz tube reactor where it was saturated with 100 mL/min of 1% NH_3/He for 1 h at room temperature. Prior to TPD, the physisorbed NH_3 was removed from the sample by purging with a 100 mL/min flow of N_2 at 100 °C. Following this step, the sample was cooled down to 50 °C, and starting from this point, the temperature was ramped to 650 °C with 5 °C/min in 100 mL/min N_2 flow. The desorption of the chemisorbed ammonia was monitored with a computer-interfaced Jasco V-570 UV/VIS/NIR spectrometer using the characteristic NH_3 band at 201 nm. The ammonia concentration was then calculated on the basis of the intensity of the characteristic band using a calibration curve. The area under the TPD curve was used for calculation of the total amount of desorbed NH_3.

IR spectra of the samples were measured with a Perkin–Elmer 1710, Fourier Transform Infrared Spectrometer at room temperature. The spectra were recorded ex situ on pellets prepared by mixing 0.5 mg of the sample with 100 mg KBr.

EPR spectra of the samples were recorded ex situ with a Bruker EMX-EPR spectrometer, operating in the X-band (Bruker ER 041 XGG Microwave Bridge) with microwave frequencies around 9.35 GHz. The measurements were performed at room temperature on samples, which were kept dry by storing them in an excicator using silica as drying agent immediately after the calcination. Data treatment was performed with WIN-EPR software provided by Bruker.

3 Results and Discussion

3.1 Characterization

XRD was recorded for all the BEA zeolite catalysts as depicted in Fig. 1 where representative examples are shown in form of the diffractogram of a H-BEA zeolite and an IS sample. The patterns clearly reveal that crystalline BEA-structured material was formed in all cases, and the XRD patterns are comparable with those reported in the literature [20–22].

The XRD patterns are characterized by sharp and broad reflections as expected for samples where an intergrowth of different BEA polymorphs has taken place [21, 22]. The diffraction patterns are similar for all the prepared zeolites including the case where iron has been introduced by isomorphous substitution.

The iron contents found by ICP-MS in the samples prepared by IWI were generally in accordance with the expected concentrations. The iron contents in the IE-sample and the IS-sample were found to be 2.3 and 1.2 wt%, respectively.

N_2 desorption and adsorption experiments were performed to investigate the porosity of the calcined BEA zeolites, and the effect on the porosity when introducing iron into the framework. Results are given in Table 1. The surface areas for all the synthesized zeolites without iron are in the range between 490 and 570 m^2/g, which is expected for standard BEA zeolites [23]. When iron is added by IWI or IE methods the surface areas decrease about 10%. In the zeolites, where iron is introduced by the IS method, the surface area is significantly lower. The decrease of the area observed for the iron containing samples might be explained by some pore blocking of the zeolite micropores by iron oxide particles. The micropore volumes are 0.205 cm^3/g for an H-BEA zeolite and 0.132 cm^3/g for an IS sample. The pore size is approximately the same, around 20–21 Å.

Table 1 Nitrogen adsorption/desorption data for the BEA zeolite prepared conventionally or via isomorphous substitution

	BET area (m^2/g)	Micropore volume (cm^3/g)	Pore size (Å)
Conv. H-BEA	562	0.205	21.5
IS	340	0.132	20.0

The N_2 adsorption and desorption isotherms are displayed in Fig. 2 for a H-BEA zeolite as well as for an isomorphous substituted sample. It is seen that the Fe-BEA catalysts exhibit a type I isotherm, which was observed for all prepared Fe-BEA samples and is typical for microporous materials such as zeolites.

The surface acidity profiles of the surfaces of the catalysts were determined by NH_3-TPD. A typical TPD profile is shown in Fig. 3, where a sample prepared by IS has been chosen as an example.

The NH_3 desorption show at least two peaks, located at 200 and 300 °C for the samples prepared with IS and around 250 and 400 °C for IWI samples. The peak at low temperature can be assigned to physisorbed NH_3 while the peak at higher temperature can be related to surface acid sites [24, 25]. The IS sample has the lowest acid content

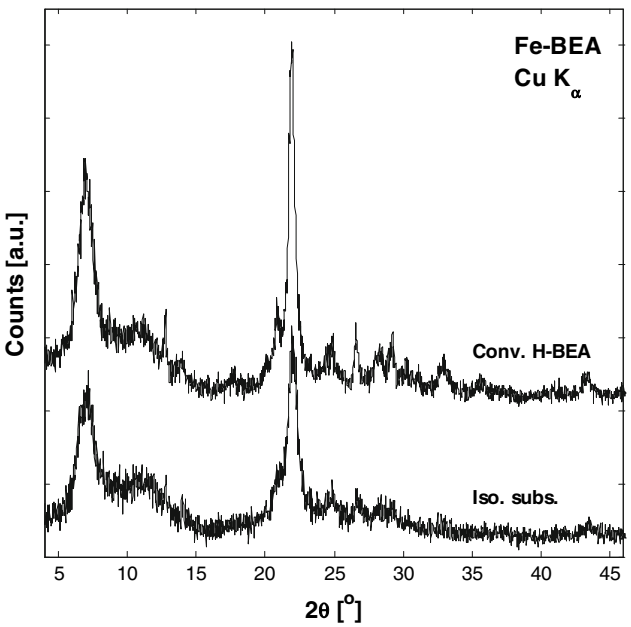

Fig. 1 XRD patterns of iron-containing BEA zeolites

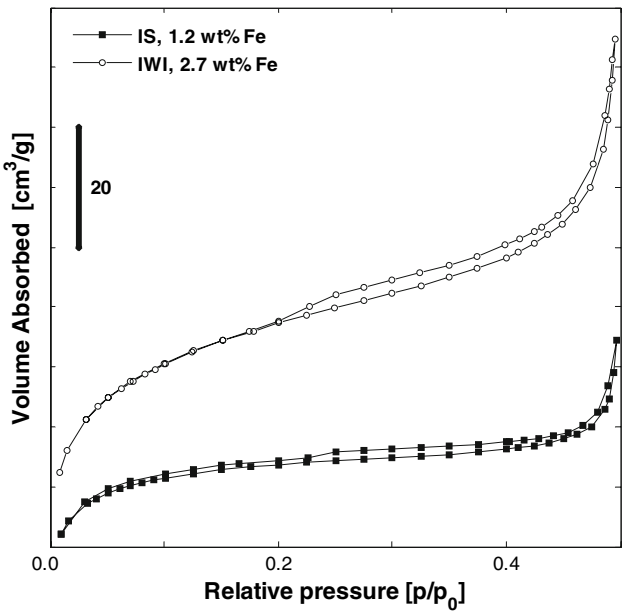

Fig. 2 Isoterms of BEA zeolites prepared by isomorphous substitution or by the conventional incipient wetness impregnation method

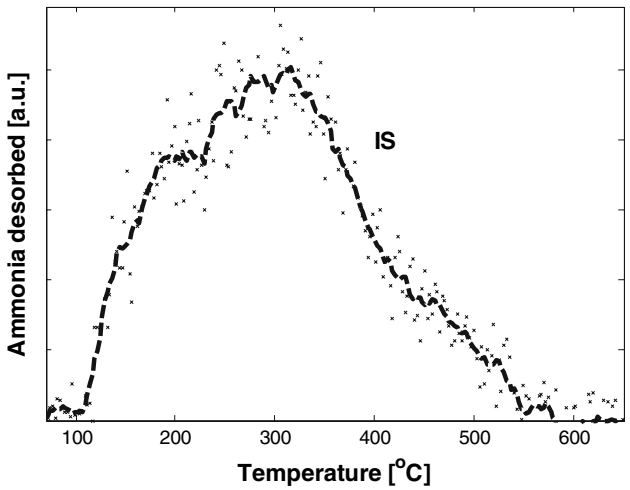

Fig. 3 Ammonia TPD profile of BEA zeolite prepared by isomorphous substitution

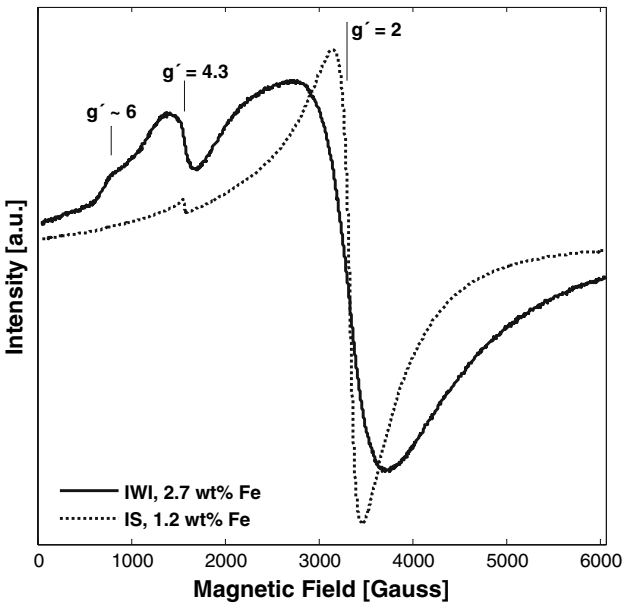

Fig. 4 Room temperature EPR spectra of selected samples

among the samples prepared, namely around 1,250 μmol/g, and the physical adsorption of NH_3 seem to be highest on these samples. The surface acidity for the IWI samples are somewhat higher, around 1,550–1,659 μmol/g. This is in accordance with observations on Fe-ZSM-5, where it was concluded that incipient wetness impregnation followed by calcination mainly leads to the formation of iron oxide species, and that the degree of ion-exchange is somewhat limited [16].

FTIR spectroscopy was employed for monitoring the hydroxyl stretching and framework vibrations in the zeolites. Hydroxyl stretches are observed at 4,000–3,200 cm^{-1} in form of a broad band with some fine structure. Several bands are expected in this area, e.g. for H-bonded silanols, iron-hydroxide stretching vibrations as well as aluminium hydroxyls. Bands originating from the framework of BEA zeolites are found between 1,250 and 450 cm^{-1} in accordance with the literature [26–28]. Traces of water were observed as well, which is expected for ambient studies of zeolite systems. Based on this, all bands can be accounted for as being Fe-BEA related, except for a few weak shoulders. Further details are thus not reported in this study.

The EPR spectra recorded at room temperature are depicted in Fig. 4. X-band EPR spectra of Fe^{3+}-containing zeolites usually consist of three major signals, one signal observed at approximately $g' = 4.3$, a broad signal at $g' = 2.0$–2.3, and a sharp signal at $g' = 2.0$ [29]. The commonly accepted assignments of the three signals is: framework iron (tetrahedral lattice Fe^{3+} ions), iron in interstitial oxide or hydroxide phases, and iron in cation-exchange sites (isolated Fe^{3+} ions, dimers or FeO_x oligomers), respectively. A fourth signal might be observed at $g' = 6$ and can be assigned to isolated Fe^{3+} ions in higher coordination [29, 30]. Figure 4 shows EPR spectra of samples prepared by IS and IWI. The differences between Fe^{3+} species in samples prepared by IWI and IS are clearly seen in the EPR spectra.

The IWI sample with 2.7 wt% Fe is dominated by the low field signals at $g' = 6$ and 4.3, as well as the broad 2.0–2.3 signal attributed to oxide or clustered species with antiferromagnetic interactions between the Fe-ions [31]. This suggests a distribution of Fe-species by IWI impregnated samples, such that a significant amount is dispersed as isolated Fe^{3+} in both octahedral and tetrahedral coordination, while the rest is present as oxide, hydroxide or clustered species.

The IS-prepared sample exhibits relatively little absorbance at low field, and it is dominated by a rather symmetric and more narrow ($\Delta H_{p-p} = 200$ Gauss) band at $g' = 2.0$. This is attributed to isolated Fe^{3+} ions, dimers or small clusters. Furthermore a peak at $g' = 4.3$ originating from tetrahedral framework Fe^{3+} is observed. Since the other bands are less dominant or not even seen for the IS sample, it must be assumed to contain less oxides and higher coordinated iron compared to the IWI samples.

3.2 Catalytic Activity

The catalytic conversion of NO over Fe-BEA zeolites were measured in the temperature range 25–550 °C, and compared to the activity of a synthesized 3 wt% V_2O_5/TiO_2 catalyst. In Fig. 5, the SCR activities of iron-based zeolites with different iron-introduction methods are shown: IWI, IE and IS.

For all the presented SCR activities, it is seen that very high conversions are obtained at temperatures above

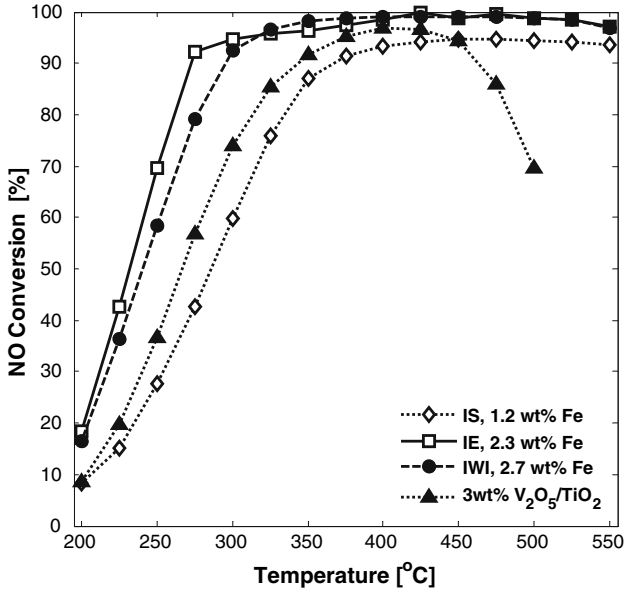

Fig. 5 Temperature dependency of the catalytic SCR activity of the BEA catalysts prepared by different methods

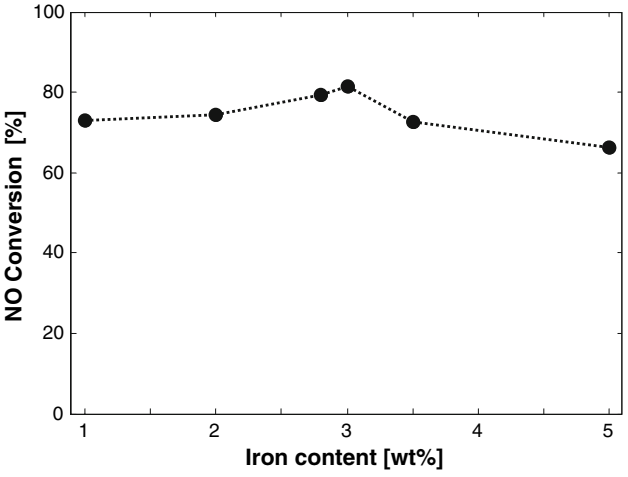

Fig. 6 Dependency on SCR activity of metal content at 275 °C

~350 °C. This makes the determination of the maximum activity uncertain. However, due to a small decrease in activity of the iron-loaded zeolites at >525 °C, the maximum can be estimated to be around 450 °C, whereas the maximum for the V_2O_5/TiO_2 catalyst is at ca. 400 °C as observed previously [17] for this catalyst. Although the relative catalyst activities displayed in Fig. 5 cannot be ranked in the temperature range 350–400 °C, due to the observed high conversion, it can be done especially below 300–350 °C.

Thus, the two zeolite catalysts prepared via IE and IWI exhibit low-temperature SCR activity, almost a factor of two higher activity at 250 °C than the reference vanadium catalyst. The overall activity of the IS prepared sample is lower than the reference catalyst, and thereby the two other BEA catalysts, although higher NO_x conversion is obtained at temperatures above 450 °C, demonstrating the high-temperature activity and stability of the Fe-BEA type catalysts. It should be noted that the IS prepared sample has a lower content of iron, 1.2 wt%, whereas the catalysts prepared via IE and IWI contain 2.3 and 2.7 wt% iron, respectively.

The influence of the iron content on the SCR activity was investigated for samples prepared by IWI. In Fig. 6 this is displayed by plotting the SCR activity at 275 °C versus the iron content in the BEA zeolite. The most active catalysts prepared by IWI seem to be those containing about 3 wt% iron, although the difference in SCR activities is rather small. This is in good agreement with the EPR spectra (see "Supplement Material"), where the intensities of the peaks are of comparable dimensions indicating only small differences between the samples. However, a trend is seen between the activity and the intensities of the EPR signals. The intensities of the signals at low field ($g' = 4.3$ and $g' = 2.0$–2.2) follow the SCR activity of the samples—the higher catalytic activity the more intense the EPR signal. For the band at $g' = 4.3$ the difference in intensity is less pronounced and the signal from 2.7 wt% Fe-BEA is found to be similar to that of 3.5 wt% Fe-BEA, except from this, the trend is the same as for the other bands.

The fact that the activity is not highly influenced by the iron-content, suggests that the difference in metal loading cannot account for the notable difference in SCR activity between the IWI samples compared to the IS samples. The lower activity of the IS samples might be explained by a non-optimal iron distribution, which the EPR spectra (see Fig. 4) suggests as well. The type of iron species present is clearly different for this IS sample than for the other samples. Thus, the IS preparation method described above does not lead to the iron species required for high SCR activity.

Alternatively the somewhat lover SCR activity can be due to the lower surface acidity of the IS prepared samples compared to the IWI sample. The surface acidity plays an essential role in the absorption of ammonia and is thus imperative for a high SCR activity [5].

The difference in micropore volume for the IS prepared catalysts compared to the BEA zeolite (cf. Table 1) have previously been shown in literature not to effect the zeolites activity in the SCR reaction significantly [15]. The contrast in microporosity of the impregnated BEA and the IS prepared catalysts can thus not explain the activity difference between the IS and IWI prepared samples displayed Fig. 5.

By comparing the SCR activity of the Fe-BEA catalysts with Fe-ZSM-5 and Fe-ZSM-12 [17], as illustrated in Fig. 7, it is evident that BEA is more promising as zeolite

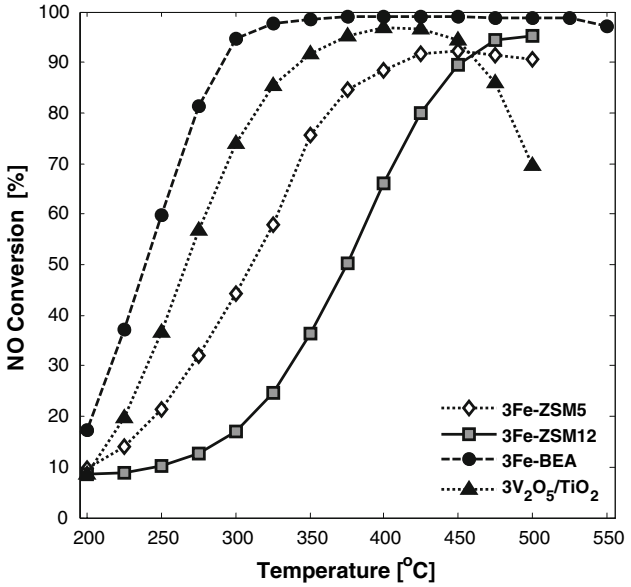

Fig. 7 Comparison of SCR activities of 3 wt% iron in different zeolites

component for iron-based SCR catalysts than the ZSM-5 and especially ZSM-12 systems. The reason for this is likely to be found in the difference in the zeolite structures. ZSM-12 has only straight channels in one dimension (5.6 × 6.0 Å) while ZSM-5 has both straight (5.3 × 5.6 Å) and sinusoidal (5.1 × 5.5 Å) channels. Thus ZSM-5 has smaller pores than ZSM-12, but a more open structure. BEA on the other hand has, with its three dimensional pore system and large channels, a more open structure than both of the ZSM zeolites. BEA has straight channels (6.6 × 6.7 Å) as well as sinusoidal (5.6 × 5.6 Å) channels. The open structure of BEA is expected to improve the diffusion through the zeolite and thereby increasing the SCR activity, as observed experimentally. It should be mentioned that all three zeolites have been prepared with the same Si/Al ratio of 50, and that they all contains approximately 3 wt% iron, introduced to the zeolites by IWI, in order to compare them in a fair manner. The above presented activity data gives reason to believe that the BEA system can play a considerable role in the future development of the SCR catalyst system.

4 Conclusion

A series of iron-containing BEA-zeolites have been prepared and compared with analogous iron containing ZSM-5 and ZSM-12. We have found that Fe-BEA catalysts in general are promising catalysts for the NH_3-SCR reaction and exhibit high catalytic activity in a broad temperature interval compared to the other zeolites and to the V_2O_5/TiO_2 catalysts. The Fe-BEA catalysts were prepared in multiple ways and all of these lead to relatively high SCR activity. However, it seems that the most active Fe-BEA catalysts for the SCR process are obtained by simple impregnation or by ion exchange. The isomorphous substitution results in catalysts with significant lower SCR activity than the other two types of preparation methods. In order to optimize the BEA catalyst in terms of iron loading, different iron amounts were incorporated in the zeolite using IWI. It was found that the 3 wt% Fe-BEA catalyst gave slightly higher SCR activity than the other iron loadings. It is expectable that Fe-containing zeolite catalysts, especially the Fe-BEA, can be improved even further by optimization. Due to the high activity of Fe-BEA and the possibility of further improvement the catalyst system might have potential for the NO_x-removal in future automotive applications.

Acknowledgments The Center for Sustainable and Green Chemistry is sponsored by the Danish National Research Foundation. Support from Energinet.dk (project PSO-FU7318) is gratefully acknowledged. We thank Dr. Søren Brik Rasmussen at Instituto de Catálisis y Petroleoquímica, Consejo Superior de Investigaciones Científicas, for recording the EPR spectra.

References

1. Klingstedt F, Arve K, Eranen K, Murzin DY (2006) Acc Chem Res 39:273
2. Hauck P, Jentys A, Lencher JA (2007) Appl Catal B Environ 70:91
3. Elmøe TD, Sørensen RZ, Quaade U, Christensen CH, Nørskov JK, Johannessen T (2006) Chem Eng Sci 61:2618
4. Armor JN (1995) Catal Today 26:99
5. Forzatti P (2001) Appl Catal A Gen 222:221
6. Busca G, Lietti L, Ramis G, Berti F (1998) Appl Catal B Environ 18:1
7. Delahay G, Mauvezin M, Coq B, Kieger S (2001) J Catal 202:156
8. Pieterse JAZ, Bonneveld S (2007) Appl Catal B Environ 73:327
9. Chen H-Y, Wang X, Sachtler WMH (2000) Appl Catal A Gen 194–195:159
10. Kiegel S, Delehay G, Coq B (2000) Appl Catal B Environ 25:1
11. Walker AP (1995) Catal Today 26:107
12. Sullivan JA, Cunningham J, Morris MA, Keneavey K (1995) Appl Catal B Environ 7:137
13. Ma A-Z, Muhler M, Grünert W (2000) Appl Catal B Environ 27:37
14. Long RQ, Yang RT (2000) J Catal 194:80
15. Pérez-Ramírez J, Groen JC, Brückner A, Kumar MS, Bentrup U, Debbagh MN, Villaescusa LA (2005) J Catal 232:318
16. Kustov AL, Egeblad K, Kustova M, Hansen TW, Christensen CH (2007) Top Catal 45:159
17. Kustov AL, Hansen TW, Kustova M, Christensen CH (2007) Appl Catal B Environ 76:311
18. Halsey G (1948) J Chem Phys 16:931
19. Brunauer S, Emmett PH, Teller E (1938) J Am Chem Soc 60:309
20. Higgins JB, LaPierre RB, Schlenker JL, Rohrman AC, Wood JD, Kerr GT, Rohrbaugh WJ (1988) Zeolites 8:446
21. Lu B-W, Jon H, Kanai T, Oumi Y, Itabashi K, Sano T (2006) J Mater Sci 41:1861
22. Newsam JM, Treacy MMJ, Koetsier WT, De Gruyter CB (1988). Proceedings of the Royal Society of London, Series A, Mathematical and Physical Sciences 420:375

23. Schoeman BJ, Babouchkina E, Mintova S, Valtchev VP, Sterte J (2001) J Por Mater 8:13
24. Hegde SG, Kumar R, Bhat RN, Ratnasamy P (1989) Zeolites 9:231
25. Camiloti AM, Jahn SL, Velasco ND, Moura LF, Cardoso D (1999) Appl Catal A Gen 182:107
26. Kumar R, Thangaraj A, Bhat RN, Ratnasamy P (1990) Zeolites 10:85
27. Armaroli T, Trombetta M, Alejandre AG, Solis JR, Busca G (2000) Phys Chem Chem Phys 2:3341
28. Díaz R, Macías S, Cázares E (2005) J Sol-Gel Sci Technol 35:13
29. Goldfarb D, Bernardo M, Strohmaier KG, Vaughan DEW, Thomann H (1994) J Am Chem Soc 116:6344
30. Dzwigaj S, Janas J, Machej T, Che M (2007) Catal Today 119:133
31. Schwidder M, Kumar MS, Klementiev KV, Pohl MM, Brückner A, Grünert W (2005) J Catal 231:314